COMPLEX IMPEDANCE RESPONSE OF Al/V_2O_5–P_2O_5/Al STRUCTURES*

J. Šimočková, P. Mikloš, V. Šály[1]

Slovak University of Technology, Faculty of Electrical Engineering and Information Technology, Ilkovičova 3, SK-81219 Bratislava, Slovak Republic

Received 18 July 2000, in final form 28 September 2000, accepted 29 September 2000

Glass samples of composition 30 mol % of P_2O_5 and 70 mol % V_2O_5 were used in this study. They were prepared by the usual melt–quench method. The electrical conductance and capacitance were measured over the frequency range 1 Hz to 1 MHz. Measurements were performed in the temperature range between 303 and 403 K. The dielectric and complex impedance response of the measured structure is discussed. The equivalent circuit was proposed and its parameters calculated. A good agreement between proposed double–layer physical model and parameters of equivalent electrical circuit was obtained.

PACS: 72.80.Ng

1 Introduction

Electrical conducting glasses have attracted much interest in the field of solid-state chemistry and materials science. Vanadium pentoxide V_2O_5 is known to have a structure composed of VO_5 pyramids. Several vanadate (V_2O_5) glasses show a semiconductive behaviour with the electrical conductivity σ of the order of about 10^{-3} to 10^{-5} Sm^{-1} which is known to be due to the electron hopping between V^{4+} to V^{5+} ions, existing in the structure of the glass. The mechanism of semiconductivity was explained by a small polaron hopping theory. The strong interaction of electrons with ions produces the localisation and the formation of polarons in the vanadium glasses.

Glasses containing transition metal oxides (TMO) are interesting for their possible application in threshold, memory switching, and others. TMO glasses based on glass network formers such as P_2O_5, TeO_2, Bi_2O_3 etc. have been studied [1–3]. Vanadium glasses are n−type semiconductors for low value of V^{4+}/V^{5+} ratio. Some characterisation of electrical and dielectric properties of V_2O_5–P_2O_5 glass in the structure metal-semiconductive glass-metal was given in our previous papers [4–6].

There are several questions regarding the frequency dependencies of electrical properties of TMO glasses and complex quantities, such as *ac* conductivity, permittivity or impedance (both, their real and imaginary parts). Dependencies as a function of frequency or temperature are

*Presented at the Workshop on Solid State Surfaces and Interfaces II, Bratislava, Slovakia, June 20 – 22, 2000.

[1] E-mail address: vsaly@elf.stuba.sk

often investigated. The polarisation effects at the electrodes and the presence of mechanisms which give rise to frequency dependent impedance terms often lead to a masking of the actual material parameters (conductivity, permittivity). The problem can be solved by measuring the *ac* electrical response over a wide range of frequencies and analysing the data using the technique of complex plane analysis [7–10].

Many observed dielectric responses, measured on particular dielectric material lead to the distribution of relaxation times τ around the midpoint τ_0. The (relative) complex dielectric permittivity ϵ^* behaviour would be then described by the equation [11]

$$\epsilon^* - \epsilon_\infty = \frac{\epsilon_s - \epsilon_\infty}{1 + (j\omega\tau_0)^{1-\beta}} \tag{1}$$

where $\beta\pi/2$ is the angle between the real axis and the line to the centre of the circle from the high frequency intercept at the Cole-Cole plot, ϵ_s and ϵ_∞ are the static and optic value of permittivity, respectively and j is the imaginary unit. For $\beta \to 0$ the relaxation process reduces to Debye relaxation.

AC measurements are particular by the measurements and analysis of some or all of the four quantities, Z^* (complex impedance), Y^* (complex admittance), ϵ^* (dielectric permittivity), M^* (complex electric modulus). Investigated quantities are presented as a plot of the imaginary part versus real part of these functions. The form of the complex impedance may be generalised [12] to

$$Z^* = Z' - jZ'' \tag{2}$$

with other related complex quantities defined similarly.

Impedance data represented by experimentally obtained simultaneous parallel equivalent values R_p, C_p (or series equivalent values R_s, C_s) actually represent a complex network. Although all the complex plane plots are derived from the same measured data, each type of representation has its own advantages in particular circumstances. Information at high frequencies is better highlighted by admittance and permittivity plots while impedance and modulus plots provide better low frequency description [12, 13].

It is well known that the differential equations which describe diffusion are identical to those which describe the propagation of electrical signal down a resistive/capacitate branched transmission line. It was pointed out that the branched transmission line exhibits constant phase behaviour [14, 15] and therefore is an electric equivalent of the constant phase element (CPE). The constant phase element has the form

$$Z_{CPE} = Z_0(j\omega)^{-\alpha} \tag{3}$$

where Z_0 and α are both real parameters. Value of coefficient α lies between 0 and 1. CPE modified Debye circuit leads to an exponential distribution of activation energies.

Except of dielectric material itself an electrode/dielectric interface modifies the impedance response of measured structure. Thermodynamically and kinetically one can distinguish between electrode/dielectric interfaces which pass a steady state current and those which are ideally polarisable or blocking to charge transfer reactions.

2 Sample preparation and measurement

Glass samples of composition 30 mol % of P_2O_5 and 70 mol % V_2O_5 were used in this study. They were prepared by the usual melt–quench method. CuO as a doping admixture was added to these fundamental constituents. This mixture was homogenised and melted in a furnace at 900 °C for 3 hours. After melting the mixture was poured out on a nonmagnetic steel plate so that the sheet samples had the thickness up to 1.1 mm. To avoid internal strains, the samples were annealed at 300 °C for 1 hour. Annealed samples were ground off and polished so that their thickness was between 0.7 and 1.0 mm. Finally, Al electrodes were (vacuum) deposited on both sides of samples. The prepared electrodes were of circular shape with the diameter about 7 mm. The electrical conductance and capacitance were measured. Data were acquired using the *Solartron* 1260 frequency response analyser in voltage drive mode employing a linear sweep over the frequency range 1 Hz to 1 MHz. The amplitude of measuring ac voltage signal was 0.5 V. PC computer was used for data acquisition. Connection to the *Solartron* was performed by screened coaxial cable (0.5 m length). Measurements were performed in the temperature range between 303 and 403 K in the thermostat chamber in air. The temperature of the sample was kept constant within an accuracy of ± 0.5 K. Amorphous nature of the samples was confirmed by X-ray diffraction method.

3 Results and discussion

The real and imaginary parts of complex permittivity and complex impedance were calculated from measured values of capacitance C_p and conductance G_p. An equivalent electrical circuit was proposed to characterise the electric behaviour of prepared samples.

3.1 Dielectric properties

Oxide glasses are characterised by marked dielectric relaxation processes [1, 3, 5] caused not only by bulk polarisation within the material but also by an interfacial effect at the electrode surface – the barrier effect which arises on the contact between the glass and metallic electrodes. The polarisation in oxide glasses occurs due to the presence of ions with different valencies which enables the thermal activation of electrons and is manifested by their hopping between the ions. Formation of thin layer on the surface of a material with electrophysical properties different from those of bulk properties can be caused by other factors, e.g. thermal processing. The system material/electrodes can be evaluated as conductive or dielectric system with a distribution of activation energies or distribution of relaxation times.

The examples of frequency dependencies of real and imaginary parts of complex permittivity ϵ' and ϵ'' are in Fig. 1 and Fig. 2, respectively. One can recognise the dielectric response of system with superposition of two different polarisation processes. The real parts of complex permittivity ϵ' limit to the ϵ_s – static value, at low frequency end of the $\epsilon'(f)$ plot and to the ϵ_∞ – optical value, at high frequency end.

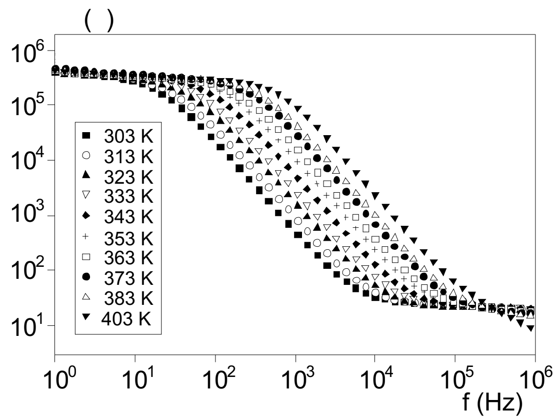

Fig. 1. Frequency dependencies of real part of complex permittivity at different temperatures.

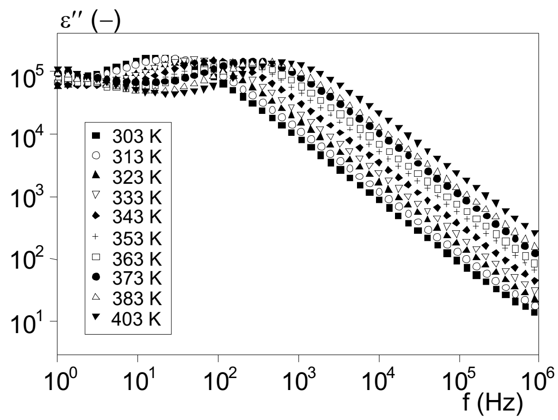

Fig. 2. Frequency dependencies of imaginary part of complex permittivity at different temperatures.

3.2 Complex impedance analysis

The example of the measured complex impedance plots of V_2O_5–P_2O_5 glasses (so–called Nyquist diagram) at different temperatures is shown in Fig. 3.

In an ideal case the plotted curves of the complex quantities (imaginary part plotted *vs* real part when the frequency of measured signal is changing) are semicircular arcs or straight lines. The shape of the curves depends on the character of conductivity and polarisation processes in investigated material or material structure. The comparison of the response of discrete elements – resistors and capacitors – connected in series or parallel when the frequency of the electric signal is changing, leads to the use of an equivalent circuit. Measured values were fitted using the equivalent electrical circuit in Fig. 4. The accuracy of the fitting procedure is visible in Fig. 5.

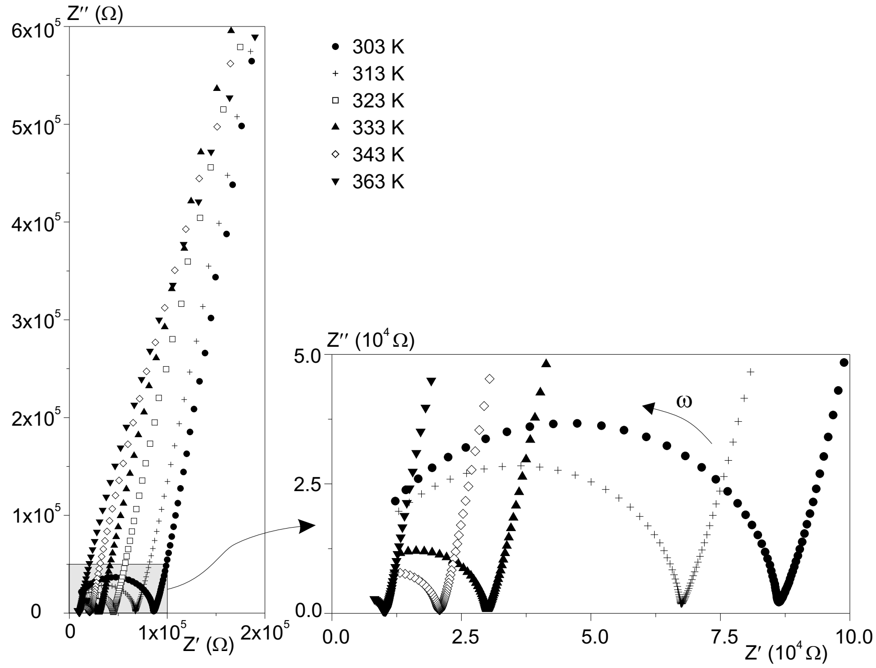

Fig. 3. Complex impedance diagram of the structure Al/V$_2$O$_5$–P$_2$O$_5$/Al measured at different temperatures. The "bulk" arcs become smaller with increasing temperature.

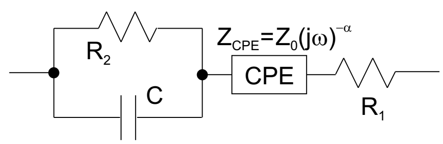

Fig. 4. Equivalent electrical circuit of the dielectric with two relaxation processes.

The equation

$$Z^*(\omega) = R_1 + \frac{R_2}{1 + j\omega\tau} + Z_{CPE} \tag{4}$$

where $\tau = R_2 C$ and Z_{CPE} obeys the relation (3), was used to approximate the complex impedance response of measured samples.

Two parts of complex impedance diagram – arc and straight line – shown in Fig. 3 are the result of two different effects – conductive and polarisation. As it was shown and discussed in our previous papers [4, 5], two different effects determine the electrical behaviour of studied glass — the bulk conductivity as a result of electron hopping and the effect of the near-electrode

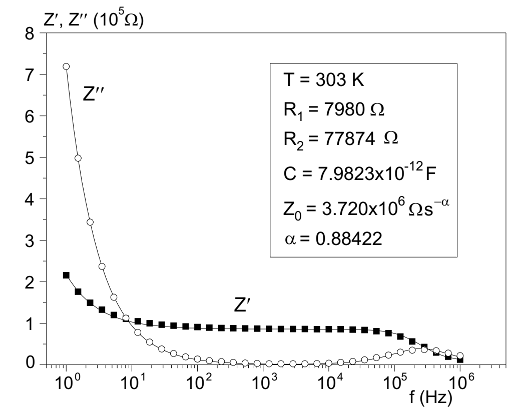

Fig. 5. Measured (symbols) and calculated (solid lines) data of complex impedance. Parameters of equivalent electric circuit (Fig. 4) are given in inset.

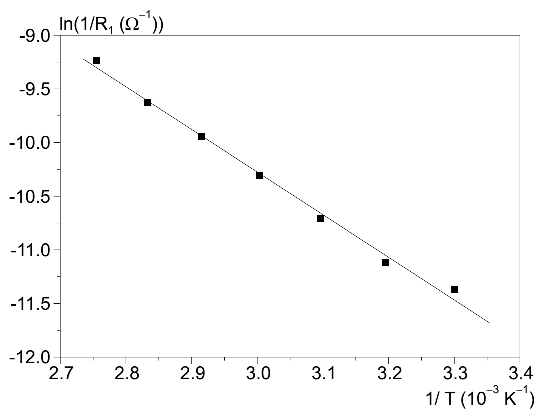

Fig. 6. Arrhenius plot of extrapolated *dc* conductance $(1/R_1)$ of Al/V_2O_5–P_2O_5/Al structure.

process. The line (the low frequency part of the Nyquist diagram) in Fig. 3 reflects the electrode – semiconductive interface properties. With regard to the behaviour of electric charge in the case of diffusion process, this part of diagram is generally in an ideal case a straight line and the CPE can characterize it.

The activation energy of *dc* conductance was calculated using resistance values in the minimums in Fig. 3. The Arrhenius plot has a linear form (Fig. 6) and $E_A = 0.34$ eV was calculated. This value is in very good agreement with published activation energies of V_2O_5–P_2O_5 structure [16].

Temperature dependencies of some chosen values of the fitted parameters of equivalent cir-

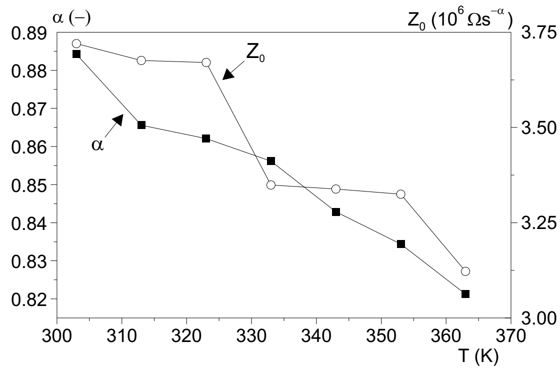

Fig. 7. The temperature dependencies of the fitted values of the parameters Z_0 and α. The solid lines are used as eye–guides.

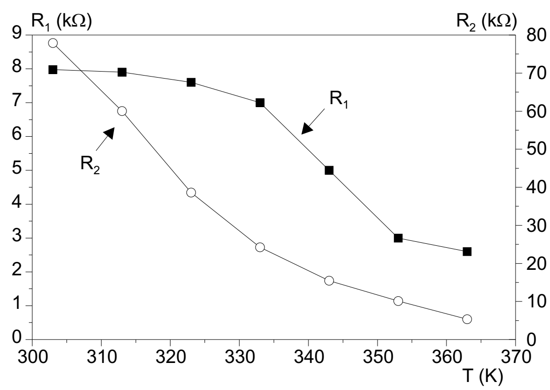

Fig. 8. Temperature dependencies of the fitted parameter R_1, R_2 of the equivalent circuit.

cuit are given in Figs. 7 and 8. The value of equivalent capacitance increases with increasing of the temperature. The output energy of metals is temperature almost independent while the output energy of semiconductors is temperature dependent. The concentration of electric charge in semiconductive material is temperature dependent, too. This fact results in the affecting the space charge region thickness of interfacial layer between semiconductor and metal electrode by temperature. The capacitance of the bulk and a near-electrode layer properties are influenced in such a way too.

Parameter α generally varies between 0 and 1, characterising the CPE properties. For $\alpha = 0$ CPE shows pure resistance character. In another limit case (for $\alpha = 1$) CPE is pure capacitance. In the case of Al/V_2O_5–P_2O_5/Al structure at mentioned conditions as it is seen in Fig. 7, α is larger than 0.82.

4 Conclusion

The design of equivalent electrical circuit (Fig. 4) started from assumption that near–electrode layers reach much more higher resistivity values than bulk material itself. Therefore, one can consider the investigated Al/V_2O_5–P_2O_5/Al structure as a layer capacitor with significantly different resistivity of each layer. Extremely high values of real part ϵ' of dielectric permittivity at low frequencies validate that mentioned layers of thickness about $10^{-8}-10^{-7}$ m [17] are present. In proposed equivalent circuit resistance R_1 represents resistivity of bulk material. Parallel connection of R_2-C elements in the equivalent electrical circuit reflects properties of near-electrode layer and CPE element corresponds to polarisation processes in Al/V_2O_5–P_2O_5/Al structure with adequate distribution of relaxation times. Numerical values of R_1 and R_2 as well as α and R_1, R_2 temperature dependencies (Figs. 7, 8) confirm assumptions about proposed circuit and they are in good agreement with designed model. Decreasing of R_1 and R_2 values with increasing temperature corresponds to the behaviour of semiconductive bulk material or near–electrode layer, respectively.

Acknowledgement. This work has been supported by VEGA – Scientific Grant Agency of Ministry of Education of Slovak Republic – under project No. 1/7606/20.

References

[1] M. Sayer, A. Mansingh, J. M. Reyes, G. Rosenblatt: *J. Appl. Phys.* **42** (1971) 487

[2] N. F. Mott, E. A. Davies: *Electronic processes in noncrystalline materials*, Clarendom Press, Oxford 1971

[3] P. Mikloš, V. Olah, J. Doupovec: *J. Non-Cryst. Sol.* **209** (1997) 137

[4] P. Mikloš, V. Šály, J. Šimočková: in *Proc. ISSE'98, 21st International Spring Seminar on Electronics Technology*, Neusiedl am See, Austria, May 1998, p. 34

[5] J. Šimočková, P. Mikloš, V. Šály: in *Proc. ISSE'99, 22nd International Spring Seminar on Electronics Technology*, Dresden, Germany, May 1999, p. 246

[6] P. Mikloš, J. Doupovec: *J. Mat. Sci.* **32** (1997) 529

[7] S. Mandal, A. Ghosh: *Philosophical Magazine B* **79** (1999) 1175

[8] M. Hartmanová, F. Kundracik, J. Schneider, T. V. Oreshnikova: *Acta Physica Slovaca* **49** (1999) 419

[9] K. Mizumoto, S. Hayashi: *Solid State Ionics* **127** (2000) 241

[10] M. Rapoš, M. Ružinský, Š. Luby, J. Červenák: *Thin Solid Films* **36** (1976) 103

[11] K. S. Cole, R. H. Cole: *J. Chem. Phys.* **9** (1941) 341

[12] A. Hooper: in *Proc. of the NATO Advanced Study Institute*, Alcabidechte, Portugal, 1984, p. 20

[13] V. Ďurman, O. Olach: *J. El. Eng.* **48** (1997) 79

[14] W. Schneider: *J. Phys. Chem.* **79** (1975) 127

[15] I. D. Raistrick: *Solid State Ionics* **18&19** (1986) 40

[16] G. N. Greaves: *J. Non-Cryst. Sol* **11** (1973) 427

[17] Š. Lányi: *J. Non-Cryst. Sol* **47** (1982) 403